Autonomous navigation system for free floating experiments in parabolic flights

Francesco Sanfedino * **Daniel Alazard** *
Gabriel Galvao-Adarme * **Ismael Vivo-Martin** *
Corentin Chauffaut * **Ervan Kassarian** * **Louis Dubois** *
Mathieu Rognant ** **Hélène Evain** ***

* *ISAE-SUPAERO, Université de Toulouse, 31055 Toulouse Cedex 4,
France (francesco.sanfedino@isae.fr, daniel.alazard@isae.fr)*
** *ONERA, 31000 Toulouse, France (mathieu.rognant@onera.fr)*
*** *CNES, 31400 Toulouse, France (Helene.Evain@cnes.fr)*

Abstract: This paper presents the development of an Extended Kalman Filter for the navigation system of a spacecraft in a parabolic flight. The algorithm blends the measurements coming from two Inertia Measurement Units, one mounted on the spacecraft and one on the baseplate of the aircraft; and a camera system connected to the baseplate as well. During the zero-g phases the attitude and position of the spacecraft in the experimental area are recovered thanks to a series of Alvar markers attached on the spacecraft casing and detected by the camera system. Results from parabolic test campaign of October 2019 are finally presented.

Keywords: Extended Kalman Filter, navigation, AR sensing, nanosatellite, parabolic flights

1. INTRODUCTION

Accepted by ESA Education Office program "Fly Your Thesis", the SCRAT-0g nanosatellite (see figure 1) built by the "Flying squirrels" team flew in Novespace's parabolic flight campaign in 2017, and demonstrated the applicability of new steering laws for a cluster of 6 nano Control Moment Gyros (CMGs) mounted on a nano-satellite as outlined by Evain et al. (2017, 2019).

Figure 1. Picture of the nano-satellite SCRAT-0g

Even though the flight was a success, the experience had not been perfect: the residual accelerations acting on the aircraft during the micro-gravity phase (20 seconds) lead to a drift of the prototype so that it bumps the net of the workspace (a cube of 2 m side) in approximately 5 to 10 seconds. To continue the experiment, the experimenters drove the nanosatellite to the center of the workspace, causing disturbances that quickly saturate the CMGs.

Following this first experience, the objective of a new CNES parabolic flight campaign in 2019 was dual: to validate new control laws for the CMG cluster as proposed in Kassarian et al. (2020) and Dubois et al. (2020); to design, size and build an additional module to control the translation of the nanosatellite, to be connected to a navigation system for on-line monitoring of the position of the spacecraft inside the experimental area. Based on this navigation system the control of the translation module aims to maintain the composite system (nanosatellite and translation module) inside the workspace while minimizing disturbances induced on the rotation motion. The scope of this paper is to present the navigation algorithm based on a classical Extended Kalman Filter (EKF) which makes the fusion of the data of two Inertia Measurements Units (IMUs) and a camera system. Vision-based algorithms are not a novelty (Simon (2006), Comellini et al. (2020)), whereas the particularity of the proposed technique is to deal at the same time with the inertial navigation for the three rotation degrees of freedom of the nanosatellite and the relative position of the nanosatellite with respect to the aircraft. This work has been realized by a group of students for their master thesis and has been implemented on a real platform in the parabolic flight campaign of October 2019. Section 2 outlines the analytical derivation of the EKF, while section 3 presents the results obtained during the zero-g experience. Section 4 finally sums up the achievements of this study and the future perspectives.

2. METHODS

2.1 Extended Kalman Filter in continuous time

Let us consider the schematic view in figure 2, that represents the spacecraft in the experimental area. Three are the reference frames to be considered:

- $\mathcal{R}_i(I; x_i, y_i, z_i)$: Earth inertial reference frame
- $\mathcal{R}_a(O; x_a, y_a, z_a)$: aircraft reference frame
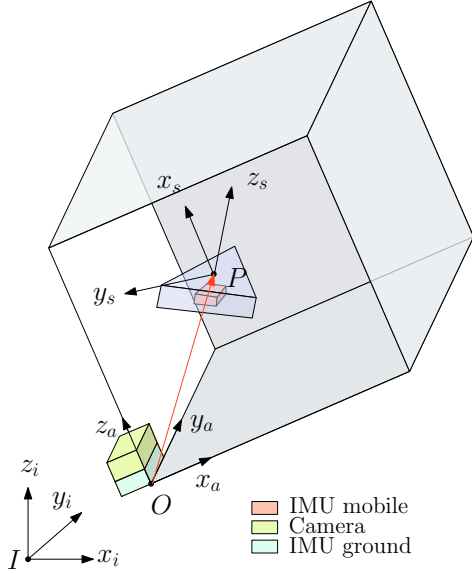- $\mathcal{R}_s(P; x_s, y_s, z_s)$: spacecraft reference frame

Figure 2. Schematic view of experiment area

The spacecraft has an embedded IMU (*IMU mobile*) and in one of the corner of the cubic experimental area there are an IMU (*IMU ground*) and a camera system both attached to the cabin floor on the baseplate.

According to figure 2 the spacecraft position vector $\overrightarrow{OP}$ can be written as:

$$\overrightarrow{OP} = \overrightarrow{IP} - \overrightarrow{IO} \tag{1}$$

The acceleration vector with respect to the inertial frame $\mathcal{R}_i$ is obtained by deriving two times (1):

$$
\left.\frac{d^2\overrightarrow{OP}}{dt^2}\right|_{\mathcal{R}_i} = \left.\frac{d^2\overrightarrow{IP}}{dt^2}\right|_{\mathcal{R}_i} - \left.\frac{d^2\overrightarrow{IO}}{dt^2}\right|_{\mathcal{R}_i} =
$$
$$
= \left.\frac{d^2\overrightarrow{OP}}{dt^2}\right|_{\mathcal{R}_a} + 2\boldsymbol{\Omega}_{\mathcal{R}_a/\mathcal{R}_i} \wedge \left.\frac{d\overrightarrow{OP}}{dt}\right|_{\mathcal{R}_a} + \dot{\boldsymbol{\Omega}}_{\mathcal{R}_a/\mathcal{R}_i} \wedge \overrightarrow{OP} +
$$
$$
+ \boldsymbol{\Omega}_{\mathcal{R}_a/\mathcal{R}_i} \wedge \left(\boldsymbol{\Omega}_{\mathcal{R}_a/\mathcal{R}_i} \wedge \overrightarrow{OP}\right) \tag{2}
$$

where $\Omega_{\mathcal{R}_a/\mathcal{R}_i}$ and $\dot{\Omega}_{\mathcal{R}_a/\mathcal{R}_i}$ are respectively the relative angular velocity and the angular acceleration between $\mathcal{R}_a$ and $\mathcal{R}_i$. By neglecting the inertial angular acceleration of the plane $\dot{\Omega}_{\mathcal{R}_a/\mathcal{R}_i}$ and projecting (2) into $\mathcal{R}_a$:

$$
\left[\left.\frac{d^2\overrightarrow{OP}}{dt^2}\right|_{\mathcal{R}_a}\right]_{\mathcal{R}_a} = \left[\left.\frac{d^2\overrightarrow{IP}}{dt^2}\right|_{\mathcal{R}_i}\right]_{\mathcal{R}_a} - \left[\left.\frac{d^2\overrightarrow{IO}}{dt^2}\right|_{\mathcal{R}_i}\right]_{\mathcal{R}_a} +
$$
$$
- 2\left[\boldsymbol{\Omega}_{\mathcal{R}_a/\mathcal{R}_i}\right]_{\mathcal{R}_a} \wedge \left[\left.\frac{d\overrightarrow{OP}}{dt}\right|_{\mathcal{R}_a}\right]_{\mathcal{R}_a} +
$$
$$
- \left[\boldsymbol{\Omega}_{\mathcal{R}_a/\mathcal{R}_i}\right]_{\mathcal{R}_a} \wedge \left(\left[\boldsymbol{\Omega}_{\mathcal{R}_a/\mathcal{R}_i}\right]_{\mathcal{R}_a} \wedge \left[\overrightarrow{OP}\right]_{\mathcal{R}_a}\right) \tag{3}
$$

The kinematic equation referred to the quaternion evolution is

$$\dot{\mathbf{q}} = \frac{1}{2}\mathbf{q} \otimes \left[\boldsymbol{\Omega}_{\mathcal{R}_s/\mathcal{R}_a}\right]_{\mathcal{R}_s} \tag{4}$$

where

$$\left[\boldsymbol{\Omega}_{\mathcal{R}_s/\mathcal{R}_a}\right]_{\mathcal{R}_s} = \left[\boldsymbol{\Omega}_{\mathcal{R}_s/\mathcal{R}_i}\right]_{\mathcal{R}_a} - \mathbf{R}_{\mathcal{R}_s\to\mathcal{R}_a}^{\mathrm{T}} \left[\boldsymbol{\Omega}_{\mathcal{R}_a/\mathcal{R}_i}\right]_{\mathcal{R}_s} \tag{5}$$

and $\mathbf{R}_{\mathcal{R}_s\to\mathcal{R}_a}$ is the rotation matrix to pass from $\mathcal{R}_s$ to $\mathcal{R}_a$. Note that the convention used for quaternion is to have the scalar part as first element of the vector and the symbol $\otimes$ denotes the quaternion product. In order to simplify the notation, the following nomenclature is used:

$$\mathbf{R}_{\mathcal{R}_s\to\mathcal{R}_a} = \mathbf{R}, \quad \left[\overrightarrow{OP}\right]_{\mathcal{R}_a} = \mathbf{r}, \quad \left[\left.\frac{d\overrightarrow{OP}}{dt}\right|_{\mathcal{R}_a}\right]_{\mathcal{R}_a} = \mathbf{v},$$

$$\left[\left.\frac{d^2\overrightarrow{OP}}{dt^2}\right|_{\mathcal{R}_a}\right]_{\mathcal{R}_a} = \dot{\mathbf{v}}, \quad \left[\left.\frac{d^2\overrightarrow{IP}}{dt^2}\right|_{\mathcal{R}_i}\right]_{\mathcal{R}_a} = \mathbf{R}\mathbf{a}_s,$$

$$\left[\left.\frac{d^2\overrightarrow{IO}}{dt^2}\right|_{\mathcal{R}_i}\right]_{\mathcal{R}_a} = \mathbf{a}_o, \quad \left[\boldsymbol{\Omega}_{\mathcal{R}_s/\mathcal{R}_i}\right]_{\mathcal{R}_s} = \boldsymbol{\omega}, \quad \left[\boldsymbol{\Omega}_{\mathcal{R}_a/\mathcal{R}_i}\right]_{\mathcal{R}_a} = \boldsymbol{\Omega} \tag{6}$$

Note that $\mathbf{r}$ and $\mathbf{q}$ are measured by the camera system, $\mathbf{a}_o$ and $\boldsymbol{\Omega}$ by the IMU on the baseplate, $\mathbf{a}_s$ and $\boldsymbol{\omega}$ by the IMU on the spacecraft.

The derivation of the EKF is fully inspired by the work of Sola (2017). The notation is the same as well to make the connection easier. The state equations to be considered for the synthesis of the EKF are then:

$$
\begin{cases}
\dot{\mathbf{r}} = \mathbf{v} \\
\dot{\mathbf{v}} = \mathbf{R}\underbrace{(\tilde{\mathbf{a}}_s - \mathbf{n}_{a_s})}_{\mathbf{a}_s} - \underbrace{(\tilde{\mathbf{a}}_o - \mathbf{n}_{a_o})}_{\mathbf{a}_o} - 2\underbrace{\left[\tilde{\boldsymbol{\Omega}} - \mathbf{b}_\Omega - \mathbf{n}_\Omega\right]_\times}_{[\boldsymbol{\Omega}]_\times}\mathbf{v} \\
\qquad - \left(\left[\tilde{\boldsymbol{\Omega}} - \mathbf{b}_\Omega - \mathbf{n}_\Omega\right]_\times\right)^2 \mathbf{r} \\
\dot{\mathbf{q}} = \frac{1}{2}\mathbf{q} \otimes \left[\underbrace{(\tilde{\boldsymbol{\omega}} - \mathbf{b}_\omega - \mathbf{n}_\omega)}_{\boldsymbol{\omega}} - \mathbf{R}^{\mathrm{T}}\left(\tilde{\boldsymbol{\Omega}} - \mathbf{b}_\Omega - \mathbf{n}_\Omega\right)\right] \\
\dot{\mathbf{b}}_\Omega = \mathbf{0} \\
\dot{\mathbf{b}}_\omega = \mathbf{0}
\end{cases} \tag{7}
$$

with $\tilde{\mathbf{a}}_s$, $\tilde{\mathbf{a}}_o$, $\tilde{\boldsymbol{\Omega}}$ and $\tilde{\boldsymbol{\omega}}$ measurements provided by the two IMUs and $\mathbf{n}_{a_s}$, $\mathbf{n}_{a_o}$, $\mathbf{n}_\Omega$ and $\mathbf{n}_\omega$ noises associated to the same sensors. Note that the measurements of the two IMUs are considered as external input signals to the system. The quantities $\mathbf{b}_\Omega$ and $\mathbf{b}_\omega$ are the bias associated to the two gyros.

The measurement equations are:

$$
\begin{cases}
\tilde{\mathbf{r}} = \mathbf{r} + \mathbf{n}_r \\
\tilde{\mathbf{q}} = \mathbf{q} + \mathbf{n}_q
\end{cases} \tag{8}
$$

with $\tilde{\mathbf{r}}$ and $\tilde{\mathbf{q}}$ direct measurements of the camera and $\mathbf{n}_r$, $\mathbf{n}_q$ associated noises. All the noises considered in this analysis are white Gaussian processes.

If we consider the state vector $\mathbf{x} = [\mathbf{r}\ \mathbf{v}\ \mathbf{q}\ \mathbf{b}_\Omega\ \mathbf{b}_\omega]^{\mathrm{T}}$, the input vector $\mathbf{u} = \left[\tilde{\mathbf{a}}_s\ \tilde{\mathbf{a}}_o\ \tilde{\boldsymbol{\Omega}}\ \tilde{\boldsymbol{\omega}}\right]^{\mathrm{T}}$, the model noise vector $\mathbf{w} = [\mathbf{n}_{a_s}\ \mathbf{n}_{a_o}\ \mathbf{n}_\Omega\ \mathbf{n}_\omega]^{\mathrm{T}}$, the measurement vector $\mathbf{y} = [\tilde{\mathbf{r}}\ \tilde{\mathbf{q}}]^{\mathrm{T}}$ and the measurement noise $\boldsymbol{\eta} = [\mathbf{n}_r\ \mathbf{n}_q]^{\mathrm{T}}$, we can rewrite (7) and (8) in the standard form for the EKF synthesis:

$$\begin{cases} \dot{\mathbf{x}} = f^c(\mathbf{x}, \mathbf{u}, \mathbf{w}) \\ \mathbf{y} = g^c(\mathbf{x}, \mathbf{u}, \boldsymbol{\eta}) \end{cases} \tag{9}$$

The state equation allows us to predict the state. The nonlinear equation can be directly used to this goal. On the other hand the estimation on the error-state $\delta\mathbf{x}$ needs a linearization of the system (9):

$$\begin{cases} \delta\dot{\mathbf{x}} = \mathbf{F}_x(\bar{\mathbf{x}}, \bar{\mathbf{u}}) \cdot \delta\mathbf{x} + \mathbf{F}_w \cdot \mathbf{w} \\ \delta\dot{\mathbf{y}} = \mathbf{G}_x(\bar{\mathbf{x}}, \bar{\mathbf{u}}) \cdot \delta\mathbf{x} + \mathbf{G}_\eta \cdot \boldsymbol{\eta} \end{cases} \tag{10}$$

where

$$\mathbf{F}_x = \left.\frac{\partial f^c}{\partial \delta\mathbf{x}}\right|_{\bar{\mathbf{x}}, \bar{\mathbf{u}}}, \mathbf{F}_w = \frac{\partial f^c}{\partial \mathbf{w}}, \mathbf{G}_x = \left.\frac{\partial g^c}{\partial \delta\mathbf{x}}\right|_{\bar{\mathbf{x}}, \bar{\mathbf{u}}}, \mathbf{G}_\eta = \frac{\partial g^c}{\partial \boldsymbol{\eta}} \tag{11}$$

with $\bar{\mathbf{x}}$ and $\bar{\mathbf{u}}$ respectively nominal state vector and nominal control vector.

Linearization   The nominal-state kinematics corresponds to the modeled system (9) without noises or perturbations:

$$\begin{cases} \dot{\bar{\mathbf{r}}} = \bar{\mathbf{v}} \\ \dot{\bar{\mathbf{v}}} = \bar{\mathbf{R}}\tilde{\mathbf{a}}_s - \tilde{\mathbf{a}}_o - 2\left[\tilde{\boldsymbol{\Omega}} - \mathbf{b}_\Omega\right]_\times \bar{\mathbf{v}} - \left(\left[\tilde{\boldsymbol{\Omega}} - \mathbf{b}_\Omega\right]_\times\right)^2 \bar{\mathbf{r}} \\ \dot{\bar{\mathbf{q}}} = \frac{1}{2}\bar{\mathbf{q}} \otimes \left[\tilde{\boldsymbol{\omega}} - \mathbf{b}_\omega - \bar{\mathbf{R}}^T\left(\tilde{\boldsymbol{\Omega}} - \mathbf{b}_\Omega\right)\right] \\ \dot{\bar{\mathbf{b}}}_\Omega = \mathbf{0} \\ \dot{\bar{\mathbf{b}}}_\omega = \mathbf{0} \end{cases} \tag{12}$$

The corresponding linearized full error-state dynamic system results:

$$\begin{cases} \delta\dot{\mathbf{r}} = \delta\mathbf{v} \\ \delta\dot{\mathbf{v}} = -\left(\left[\tilde{\boldsymbol{\Omega}} - \mathbf{b}_\Omega\right]_\times\right)^2 \delta\mathbf{r} - 2\left[\tilde{\boldsymbol{\Omega}} - \mathbf{b}_\Omega\right]_\times \delta\mathbf{v} \\ \qquad -\bar{\mathbf{R}}\left[\tilde{a}_s\right]_\times \delta\boldsymbol{\theta} - \mathbf{B}_\Omega\delta\mathbf{b}_\Omega - \mathbf{n}_{a_s} + \mathbf{n}_{a_o} - \mathbf{B}_\Omega\mathbf{n}_\Omega \\ \delta\dot{\boldsymbol{\theta}} = -\left[\tilde{\boldsymbol{\omega}} - \mathbf{b}_\omega\right]_\times \delta\boldsymbol{\theta} + \bar{\mathbf{R}}^T\delta\mathbf{b}_\Omega - \delta\mathbf{b}_\omega + \mathbf{n}_\Omega - \mathbf{n}_\omega \\ \delta\dot{\mathbf{b}}_\Omega = \mathbf{0} \\ \delta\dot{\mathbf{b}}_\omega = \mathbf{0} \end{cases} \tag{13}$$

with

$$\mathbf{B}_\Omega = \left(2\left[\bar{\mathbf{v}}\right]_\times + 2\left[\tilde{\boldsymbol{\Omega}} - \mathbf{b}_\Omega\right]_\times \left[\bar{\mathbf{r}}\right]_\times - \left[\bar{\mathbf{r}}\right]_\times \left[\tilde{\boldsymbol{\Omega}} - \mathbf{b}_\Omega\right]_\times\right) \tag{14}$$

The complete derivations of the linear velocity error $\delta\mathbf{v}$ and the attitude error $\delta\boldsymbol{\theta}$ are respectively shown in appendix A and B.

2.2 Extended Kalman Filter in discrete time

In order to implement the EKF a discretizion of sample time Δt of the system (7) is needed to propagate the state vector. If noises are neglected the discrete evolution of the state vector $\mathbf{x}_k$ is described by the set of equations:

$$\begin{cases} \hat{\mathbf{r}}_{k+1/k} = \mathbf{r}_k + \mathbf{v}_k \cdot \Delta t \\ \hat{\mathbf{v}}_{k+1/k} = \mathbf{v}_k + \left[\mathbf{R}_k\tilde{\mathbf{a}}_{s_k} - \tilde{\mathbf{a}}_{o_k} - 2\left[\tilde{\boldsymbol{\Omega}}_k - \mathbf{b}_{\Omega_k}\right]_\times \mathbf{v}_k \right. \\ \qquad\qquad \left. - \left(\left[\tilde{\boldsymbol{\Omega}}_k - \mathbf{b}_{\Omega_k}\right]_\times\right)^2 \mathbf{r}_k\right] \cdot \Delta t \\ \hat{\mathbf{q}}_{k+1/k} = \mathbf{q}_k \otimes \mathbf{q}\{\boldsymbol{\omega}_{r_k} \cdot \Delta t\} \\ \hat{\mathbf{b}}_{\Omega_{k+1/k}} = \mathbf{b}_{\Omega_k} \\ \hat{\mathbf{b}}_{\omega_{k+1/k}} = \mathbf{b}_{\omega_k} \end{cases} \tag{15}$$

with

$$\mathbf{q}\{\boldsymbol{\omega}_{r_k} \cdot \Delta t\} = \begin{bmatrix} \cos(\|\boldsymbol{\omega}_{r_k}\| \cdot \Delta t/2) \\ \frac{\boldsymbol{\omega}_{r_k}}{\|\boldsymbol{\omega}_{r_k}\|}\sin(\|\boldsymbol{\omega}_{r_k}\| \cdot \Delta t/2) \end{bmatrix} \tag{16}$$

where

$$\boldsymbol{\omega}_{r_k} = \tilde{\boldsymbol{\omega}}_k - \mathbf{b}_{\omega_k} - \mathbf{R}_k^T\left(\tilde{\boldsymbol{\Omega}}_k - \mathbf{b}_{\Omega_k}\right) \tag{17}$$

Note that an integration thanks to the Euler method is used except for the quaternion equation. This equation is obtained by forward zeroth order integration based on the development of Taylor of $\mathbf{q}(t_k + \Delta t)$ (see Sola (2017) for the derivation of this expression).

Linearization   For the error-state kinematics in discrete time, the deterministic part is integrated normally and the integration of the stochastic part (noises) results in random impulses:

$$\begin{cases} \delta\mathbf{r}_{k+1} = \delta\mathbf{r}_k + \delta\mathbf{v}_k \cdot \Delta t \\ \delta\mathbf{v}_{k+1} = \delta\mathbf{v}_k + \left(-\left(\left[\tilde{\boldsymbol{\Omega}}_k - \mathbf{b}_{\Omega_k}\right]_\times\right)^2 \delta\mathbf{r}_k + \right. \\ \qquad \left. -2\left[\tilde{\boldsymbol{\Omega}}_k - \mathbf{b}_{\Omega_k}\right]_\times \delta\mathbf{v}_k - \bar{\mathbf{R}}_k\left[\tilde{a}_s\right]_\times \delta\boldsymbol{\theta}_k - \mathbf{B}_{\Omega_k}\delta\mathbf{b}_{\Omega_k}\right) \cdot \Delta t \\ \qquad -\mathbf{n}_{a_{s_k}} + \mathbf{n}_{a_{o_k}} - \mathbf{B}_{\Omega_l}\mathbf{n}_{\Omega_k} \\ \delta\boldsymbol{\theta}_{k+1} = \bar{\mathbf{R}}_k^T\{(\tilde{\boldsymbol{\omega}}_k - \mathbf{b}_{\omega_k})\Delta t\}\delta\boldsymbol{\theta}_k + \bar{\mathbf{R}}_k^T\delta\mathbf{b}_{\Omega_k} \cdot \Delta t \\ \qquad -\delta\mathbf{b}_{\omega_k} \cdot \Delta t + \mathbf{n}_{\Omega_k} - \mathbf{n}_{\omega_k} \\ \delta\mathbf{b}_{\Omega_{k+1}} = \delta\mathbf{b}_{\Omega_k} \\ \delta\mathbf{b}_{\omega_{k+1}} = \delta\mathbf{b}_{\omega_k} \end{cases} \tag{18}$$

with

$$\mathbf{B}_{\Omega_k} = \left(2\left[\bar{\mathbf{v}}_k\right]_\times + 2\left[\tilde{\boldsymbol{\Omega}}_k - \mathbf{b}_{\Omega_k}\right]_\times \left[\bar{\mathbf{r}}\right]_\times - \left[\bar{\mathbf{r}}\right]_\times \left[\tilde{\boldsymbol{\Omega}}_k - \mathbf{b}_{\Omega_k}\right]_\times\right) \tag{19}$$

For further details about the derivation of the third equation see Appendix B.2 of Sola (2017).

Thanks to (18) we have the matrices $\mathbf{F}_x$ and $\mathbf{F}_i$ to be used for the EKF prediction:

$$\delta\mathbf{x}_{k+1} = f(\bar{\mathbf{x}}_k, \delta\mathbf{x}_k, \bar{\mathbf{u}}_k, \mathbf{i}) = \mathbf{F}_x(\bar{\mathbf{x}}, \bar{\mathbf{u}}) \cdot \delta\mathbf{x}_k + \mathbf{F}_i \cdot \mathbf{i} \tag{20}$$

with

$$\mathbf{i} = \begin{bmatrix} \mathbf{n}_{a_{s_k}} & \mathbf{n}_{a_{o_k}} & \mathbf{n}_{\Omega_k} & \mathbf{n}_{\omega_k} \end{bmatrix}^T \tag{21}$$

The EKF prediction equation are then:

$$\delta\hat{\mathbf{x}}_{k+1/k} = \mathbf{F}_x \cdot \delta\hat{\mathbf{x}}_{k/k} \tag{22}$$

$$\mathbf{P}_{k+1/k} = \mathbf{F}_x\mathbf{P}_{k/k}\mathbf{F}_x^T + \mathbf{F}_i\mathbf{Q}_i\mathbf{F}_i^T \tag{23}$$

with

$$\mathbf{F}_x = \left.\frac{\partial f}{\partial \delta \mathbf{x}}\right|_{\bar{\mathbf{x}},\bar{\mathbf{u}}} = \begin{bmatrix} \mathbf{I} & \mathbf{I}\Delta t & \mathbf{0} & \mathbf{0} & \mathbf{0} \\ -\left(\left[\tilde{\boldsymbol{\Omega}}_k - \mathbf{b}_{\Omega_k}\right]_\times\right)^2 \Delta t\ \mathbf{I} - 2\left[\tilde{\boldsymbol{\Omega}}_k - \mathbf{b}_{\Omega_k}\right]_\times \Delta t & -\bar{\mathbf{R}}_k\left[\tilde{a}_{s_k}\right]_\times \Delta t & -\mathbf{B}_{\Omega_k}\Delta t & \mathbf{0} \\ \mathbf{0} & \mathbf{0} & \bar{\mathbf{R}}_k^{\mathrm{T}}\left\{(\tilde{\boldsymbol{\omega}}_k - \mathbf{b}_{\omega_k})\,\Delta t\right\} & \bar{\mathbf{R}}_k^{\mathrm{T}}\Delta t & -\mathbf{I}\Delta t \\ \mathbf{0} & \mathbf{0} & \mathbf{0} & \mathbf{I} & \mathbf{0} \\ \mathbf{0} & \mathbf{0} & \mathbf{0} & \mathbf{0} & \mathbf{I} \end{bmatrix} \quad (24)$$

and

$$\mathbf{F}_i = \begin{bmatrix} \mathbf{0} & \mathbf{0} & \mathbf{0} & \mathbf{0} \\ -\mathbf{I} & \mathbf{I} & -\mathbf{B}_{\Omega_k} & \mathbf{0} \\ \mathbf{0} & \mathbf{0} & \mathbf{I} & -\mathbf{I} \\ \mathbf{0} & \mathbf{0} & \mathbf{0} & \mathbf{0} \\ \mathbf{0} & \mathbf{0} & \mathbf{0} & \mathbf{0} \end{bmatrix}, \ \mathbf{Q}_i = \Delta t \cdot \begin{bmatrix} \mathbf{W}_{a_s} & & & \\ & \mathbf{W}_{a_o} & & \\ & & \mathbf{W}_\Omega & \\ & & & \mathbf{W}_\omega \end{bmatrix} \quad (25)$$

The covariance associated to the model noise $\mathbf{i}$ is in fact:

$$\mathbb{E}\left[\mathbf{i}_k \mathbf{i}_{k+l}^{\mathrm{T}}\right] = \mathbf{W}_k \delta(l) \quad (26)$$

with $\delta(l) = 1$ if $l = 0$ $(\delta(l) = 0$ elsewhere$)$ and where:

$$\mathbf{W}_k = \mathbb{E}\left[\mathbf{i}_k \mathbf{i}_k^{\mathrm{T}}\right] =$$
$$= \int_0^{\Delta t} e^{\mathbf{A}^c \tau} \mathbf{F}_i \begin{bmatrix} \mathbf{W}_{a_s} & & & \\ & \mathbf{W}_{a_o} & & \\ & & \mathbf{W}_\Omega & \\ & & & \mathbf{W}_\omega \end{bmatrix} \mathbf{F}_i^{\mathrm{T}} e^{\mathbf{A}^{c\mathrm{T}} \tau} d\tau \approx$$
$$\approx \Delta t \mathbf{F}_i \begin{bmatrix} \mathbf{W}_{a_s} & & & \\ & \mathbf{W}_{a_o} & & \\ & & \mathbf{W}_\Omega & \\ & & & \mathbf{W}_\omega \end{bmatrix} \mathbf{F}_i^{\mathrm{T}} \quad (27)$$

with $\mathbf{W}_{a_s}$, $\mathbf{W}_{a_o}$, $\mathbf{W}_\Omega$ and $\mathbf{W}_\omega$ PSD associated to each sensor's noise.

Note that the last approximation holds if Δt is small with respect to the settling time of the plant.

Estimation of angular rate and acceleration Thanks to the estimation of the bias $\hat{\mathbf{b}}_\omega$ of the gyrometer on the spacecraft, we can estimate also the angular rate and acceleration of the platform:

$$\hat{\boldsymbol{\omega}}_{k+1} = \tilde{\boldsymbol{\omega}}_k - \hat{\mathbf{b}}_{\omega_k} \quad (28)$$
$$\hat{\dot{\boldsymbol{\omega}}}_{k+1} = \frac{\hat{\boldsymbol{\omega}}_{k+1} - \hat{\boldsymbol{\omega}}_k}{\Delta t} \quad (29)$$

In case the IMU on the spacecraft is not mounted exactly on its CoM but in a point M, the measurement of the acceleration $\tilde{\mathbf{a}}_s$ is then:

$$\tilde{\mathbf{a}}_{s_k} = \tilde{\mathbf{a}}_{m_k} - \left[\hat{\dot{\boldsymbol{\omega}}}_k\right]_\times \mathbf{r}_m - \left([\hat{\boldsymbol{\omega}}_k]_\times\right)^2 \mathbf{r}_m \quad (30)$$

where $\tilde{\mathbf{a}}_{m_k}$ is the acceleration measured by the IMU on the spacecraft at point M and $\mathbf{r}_m = \overrightarrow{MP}$.

Filter correction The measurement equation in discrete time is:

$$\mathbf{y}_k = h(\mathbf{x}_k) + \boldsymbol{\eta} \quad (31)$$

with $\boldsymbol{\eta}$ white Gaussian noise with covariance $\mathbf{R} = \mathbf{V}/\Delta t$, where $\mathbf{V}$ is the diagonal matrix of the PSD associated to the measurement noise.

In the analyzed system:

$$\begin{cases} \tilde{\mathbf{r}}_k = \mathbf{r}_k + \mathbf{n}_{r_k} \\ \tilde{\mathbf{q}}_k = \mathbf{q}_k + \mathbf{n}_{q_k} \end{cases} \quad (32)$$

and

$$\mathbf{V} = \mathrm{diag}\left(\mathbf{W}_r, \mathbf{W}_q\right) \quad (33)$$

with $\mathbf{W}_r$ and $\mathbf{W}_q$ PSD associated to camera's noise.

The filter correction equations are then:

$$\mathbf{K}_{k+1} = \mathbf{P}_{k+1/k} \mathbf{H}^{\mathrm{T}} \left(\mathbf{H}\mathbf{P}_{k+1/k}\mathbf{H}^{\mathrm{T}} + \mathbf{R}\right)^{-1} \quad (34)$$
$$\delta \hat{\mathbf{x}}_{k+1/k+1} = \mathbf{K}_{k+1}\left(\mathbf{y}_{k+1} - h\left(\hat{\mathbf{x}}_{k+1/k}\right)\right) \quad (35)$$
$$\mathbf{P}_{k+1/k+1} = \left(\mathbf{I} - \mathbf{K}_{k+1}\mathbf{H}\right)\mathbf{P}_{k+1/k} \quad (36)$$

where $\mathbf{H} = \left.\frac{\partial h}{\partial \delta \mathbf{x}}\right|_{\bar{\mathbf{x}}}$.

Note that the correction of the estimated state is

$$\hat{\mathbf{x}}_{k+1/k+1} = \hat{\mathbf{x}}_{k+1/k} + \delta \hat{\mathbf{x}}_{k+1/k+1} \quad (37)$$

for all the state vector except for the quaternions. In order to rebuild the estimate of the quaternion $\delta \hat{\mathbf{q}}$ from the angular position estimate $\delta \hat{\boldsymbol{\theta}}$, we use:

$$\hat{\mathbf{q}}_{k+1/k+1} = \hat{\mathbf{q}}_{k+1/k} \otimes \delta \hat{\mathbf{q}}_{k+1/k+1} \quad (38)$$

where $\delta \hat{\mathbf{q}}$ is the normalized quaternion:

$$\delta \hat{\mathbf{q}} = \begin{bmatrix} \sqrt{1 - \delta \hat{\boldsymbol{\theta}}^{\mathrm{T}} \delta \hat{\boldsymbol{\theta}}} \\ \delta \hat{\boldsymbol{\theta}}/2 \end{bmatrix} \quad (39)$$

The covariance update (36) is known to have poor numerical stability. An alternative stable expression commonly adopted in literature is the symmetric and positive definite form:

$$\mathbf{P}_{k+1/k+1} = \mathbf{P}_{k+1/k} - \mathbf{K}_{k+1}\left(\mathbf{H}\mathbf{P}_{k+1/k}\mathbf{H}^{\mathrm{T}} + \mathbf{R}\right)\mathbf{K}_{k+1}^{\mathrm{T}} \quad (40)$$

or the symmetric and positive *Joseph* form:

$$\mathbf{P}_{k+1/k+1} = \left(\mathbf{I} - \mathbf{K}_{k+1}\mathbf{H}\right)\mathbf{P}_{k+1/k}\left(\mathbf{I} - \mathbf{K}_{k+1}\mathbf{H}\right)^{\mathrm{T}} + \mathbf{K}_{k+1}\mathbf{R}\mathbf{K}_{k+1}^{\mathrm{T}} \quad (41)$$

The Jacobian $\mathbf{H}$ can be computed thanks to the chain rule:

$$\mathbf{H} = \left.\frac{\partial h}{\partial \delta \mathbf{x}}\right|_{\bar{\mathbf{x}}} = \left.\frac{\partial h}{\partial \mathbf{x}}\right|_{\bar{\mathbf{x}}} \left.\frac{\partial \mathbf{x}}{\partial \delta \mathbf{x}}\right|_{\bar{\mathbf{x}}} = \mathbf{H}_x \mathbf{X}_{\delta x} \quad (42)$$

Here, $\mathbf{H}_x$ is the standard Jacobian of $h(\bullet)$ with respect to its own argument. In this study:

$$\mathbf{H}_x = \begin{bmatrix} \mathbf{I}_3 & \mathbf{0}_{3\times 3} & \mathbf{0}_{3\times 4} & \mathbf{0}_{3\times 3} \\ \mathbf{0}_{4\times 3} & \mathbf{0}_{4\times 3} & \mathbf{I}_4 & \mathbf{0}_{4\times 3} \end{bmatrix} \quad (43)$$

$\mathbf{X}_{\delta x}$ is the Jacobian of the true state with respect to the error state:

$$\mathbf{X}_{\delta x} = \begin{bmatrix} \frac{\partial (\mathbf{r} + \delta \mathbf{r})}{\partial \delta \mathbf{r}} & & & & \\ & \frac{\partial (\mathbf{v} + \delta \mathbf{v})}{\partial \delta \mathbf{v}} & & & \\ & & \frac{\partial (\mathbf{q} \otimes \delta \mathbf{q})}{\partial \delta \boldsymbol{\theta}} & & \\ & & & \frac{\partial (\mathbf{b}_\Omega + \delta \mathbf{b}_\Omega)}{\partial \delta \mathbf{b}_\Omega} & \\ & & & & \frac{\partial (\mathbf{b}_\omega + \delta \mathbf{b}_\omega)}{\partial \delta \mathbf{b}_\omega} \end{bmatrix} \quad (44)$$

which results in all identity 3×3 blocks except for the 4×3 quaternion term $\mathbf{Q}_{\delta\theta} = \partial \left(\mathbf{q} \otimes \delta\mathbf{q} \right) / \partial\delta\boldsymbol{\theta}$. Therefore:

$$\mathbf{X}_{\delta x} = \left. \frac{\partial \mathbf{x}}{\partial \delta \mathbf{x}} \right|_{\bar{\mathbf{x}}} = \begin{bmatrix} \mathbf{I}_6 & \\ & \mathbf{Q}_{\delta\theta} \\ & & \mathbf{I}_6 \end{bmatrix} \quad (45)$$

Using the chain rule and the limit $\delta\mathbf{q} \xrightarrow[\delta\boldsymbol{\theta}\to 0]{} \begin{bmatrix} 1 \\ \frac{1}{2}\delta\boldsymbol{\theta} \end{bmatrix}$, the quaternion term $\mathbf{Q}_{\delta\theta}$ becomes (see Sola (2017)):

$$\mathbf{Q}_{\delta\theta} = \frac{1}{2} \begin{bmatrix} -q_1 & -q_2 & -q_3 \\ q_0 & -q_3 & q_2 \\ q_3 & q_0 & -q_1 \\ -q_2 & q_1 & q_0 \end{bmatrix} \quad (46)$$

3. RESULTS FROM PARABOLIC FLIGHTS

During the CNES campaign of parabolic flights in October 2019, three cameras were used in order to cover the entire experimental area and their averaged measurements were sent to the EKF camera input. When one of the measurement of any camera was not available, that particular camera was not considered in the average. An algorithm of Augmented Reality (AR) detection was developed in order to reconstruct the position and the attitude of the spacecraft with respect to each camera (see figure 3) by using the ROS `ar_track_alvar` node which uses multiple markers in a bundle fashion.

Figure 3. Spacecraft in the experimental area: view from CAM2

Post-processing of data showed some interesting results and encouraged the use of the navigation algorithm for further developments. Figures 4 and 5 respectively show position and attitude estimated during one parabola. From the lower subfigure in each of the two figures, acceleration measurements (along z-axis) gathered by the two IMUs (*ground* and *mobile*) provide the period of time when micro-gravity conditions are reached by the airplane (roughly between 27 s and 50 s). Note that spikes in *IMU mobile* acceleration measurements correspond to the impacts of the spacecraft with the net of the experimental area and the successive interaction with the operator to relocate the spacecraft in the middle of the area.

As show in figures 4 and 5, measurements from the three cameras were not available at the same time at any time. This fact means that the spacecraft was not inside the optical cone of the camera or its detection was obstructed

by the operator. This last one is the main reason why no measurements records were obtained from the first camera.

Finally figure 6 shows the first instants of the EKF integration. Until no measurements from the cameras are available, the estimation tends to diverge with a corresponding increase of the covariance. Once some measurements are available from CAM3 the filter rapidly converges and covariance drastically drops.

One possible improvement suggested by parabolic flights experience is to refine the AR acquisition algorithm in order to increase the integration time. Using full image capture from the three cameras corresponds in fact to a huge computational time that impacts on the performance of the acquisition by introducing delays. It would be interesting to test then an algorithm that takes into account only some significant points in the available point clouds.
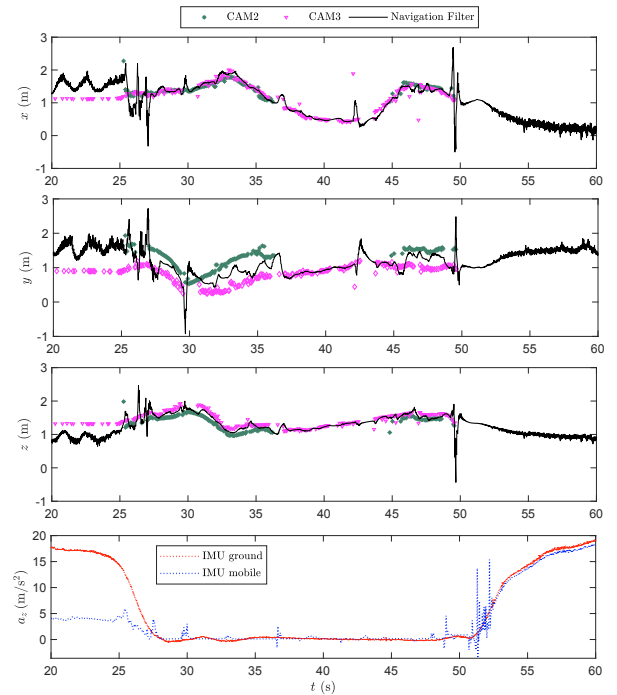

Figure 4. Navigation data in parabolic flights: position estimation

4. CONCLUSION

This paper outlined the analytical development of an Extended Kalman Filter for recovering the position and attitude of a spacecraft in a parabolic flight test. The algorithm has been implemented in a real platform and the results of the zero-g campaign have been presented. This kind of algorithm results promising for experiments in parabolic flights where keeping track of the position and attitude of a free floating object is important for the quality of gathered data. Moreover the output of the proposed navigation system can be directly used for a closed-loop synthesis if a set of actuators is available on the experimental platform.
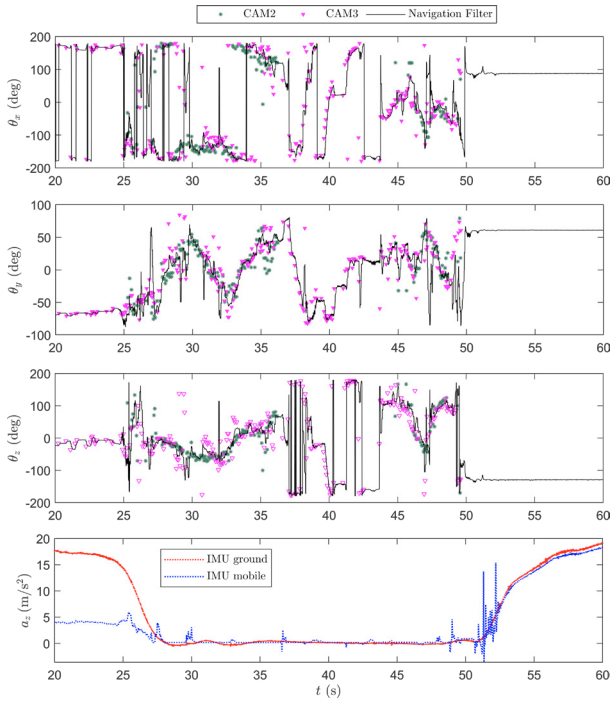
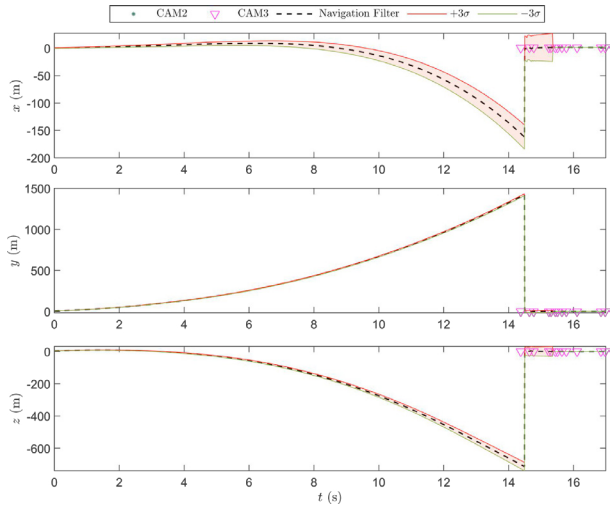Figure 5. Navigation data in parabolic flights: attitude estimation

Figure 6. Navigation data in parabolic flights: covariance in position estimation

Appendix A. THE LINEAR VELOCITY ERROR DERIVATION

This derivation is entirely inspired to the work Sola (2017). We consider the following relations:

$$\mathbf{R} = \bar{\mathbf{R}}\left(\mathbf{I} + [\delta\boldsymbol{\theta}]_\times\right) + \mathcal{O}\left(||\delta\boldsymbol{\theta}||^2\right) \qquad (A.1)$$

$$\dot{\mathbf{v}} = \bar{\mathbf{R}}\bar{\mathbf{a}}_s - \bar{\mathbf{a}}_o - 2\left[\bar{\boldsymbol{\Omega}}\right]_\times \bar{\mathbf{v}} - \left(\left[\bar{\boldsymbol{\Omega}}\right]_\times\right)^2 \bar{\mathbf{r}} \qquad (A.2)$$

where (A.1) is the small-signal approximation of the true value $\mathbf{R}$ and in (A.2) we rewrote the second equation in (12) but introducing $\bar{\mathbf{a}}_s$, $\bar{\mathbf{a}}_o$, $\bar{\boldsymbol{\Omega}}$, $\delta\mathbf{a}_s$, $\delta\mathbf{a}_o$ and $\delta\boldsymbol{\Omega}$ defined as the large- and small-signal accelerations and angular speed in body frame:

$$\begin{cases} \bar{\mathbf{a}}_s \triangleq \tilde{\mathbf{a}}_s \\ \delta\mathbf{a}_s \triangleq -\mathbf{n}_{a_s} \end{cases} \qquad \begin{cases} \bar{\mathbf{a}}_o \triangleq \tilde{\mathbf{a}}_o \\ \delta\mathbf{a}_o \triangleq -\mathbf{n}_{a_o} \end{cases} \qquad \begin{cases} \bar{\boldsymbol{\Omega}} \triangleq \tilde{\boldsymbol{\Omega}} - \mathbf{b}_\Omega \\ \delta\boldsymbol{\Omega} \triangleq -\delta\mathbf{b}_\Omega - \mathbf{n}_\Omega \end{cases}$$
$$(A.3)$$

The true accelerations $\mathbf{a}$ in the plane frame can be written as a composition of large- and small-signal terms:

$$\mathbf{a} = \mathbf{R}\left(\bar{\mathbf{a}}_s + \delta\mathbf{a}_s\right) - \left(\bar{\mathbf{a}}_o + \delta\mathbf{a}_o\right) - 2\left[\bar{\boldsymbol{\Omega}} + \delta\boldsymbol{\Omega}\right]_\times \left(\bar{\mathbf{v}} + \delta\mathbf{v}\right)$$
$$- \left(\left[\bar{\boldsymbol{\Omega}} + \delta\boldsymbol{\Omega}\right]_\times\right)^2 \left(\bar{\mathbf{r}} + \delta\mathbf{r}\right)$$
$$(A.4)$$

The true acceleration $\dot{\mathbf{v}}$ in (9) can be written in two different forms (left and right developments) as done in Sola (2017) by neglecting all the second-order terms:

$$\dot{\bar{\mathbf{v}}} + \delta\dot{\mathbf{v}} = \bar{\mathbf{R}}\left(\mathbf{I} + [\delta\boldsymbol{\theta}]_\times\right)\left(\bar{\mathbf{a}}_s + \delta\mathbf{a}_s\right) - \left(\bar{\mathbf{a}}_o + \delta\mathbf{a}_o\right)$$
$$- 2\left[\bar{\boldsymbol{\Omega}} + \delta\boldsymbol{\Omega}\right]_\times \left(\bar{\mathbf{v}} + \delta\mathbf{v}\right) - \left(\left[\bar{\boldsymbol{\Omega}} + \delta\boldsymbol{\Omega}\right]_\times\right)^2 \left(\bar{\mathbf{r}} + \delta\mathbf{r}\right)$$
$$(A.5)$$

The development of the left term is:

$$\dot{\mathbf{v}} = \bar{\mathbf{R}}\bar{\mathbf{a}}_s - \bar{\mathbf{a}}_o - 2\left[\bar{\boldsymbol{\Omega}}\right]_\times \bar{\mathbf{v}} - \left(\left[\bar{\boldsymbol{\Omega}}\right]_\times\right)^2 \bar{\mathbf{r}} + \delta\dot{\mathbf{v}} \qquad (A.6)$$

and the development of the right term is:

$$\dot{\mathbf{v}} = \bar{\mathbf{R}}\bar{\mathbf{a}}_s + \bar{\mathbf{R}}\delta\mathbf{a}_s + \bar{\mathbf{R}}[\delta\boldsymbol{\theta}]_\times \bar{\mathbf{a}}_s + \bar{\mathbf{R}}[\delta\boldsymbol{\theta}]_\times \delta\mathbf{a}_s - \bar{\mathbf{a}}_o - \delta\mathbf{a}_o$$
$$- 2\left[\bar{\boldsymbol{\Omega}}\right]_\times \bar{\mathbf{v}} - 2[\delta\boldsymbol{\Omega}]_\times \bar{\mathbf{v}} - 2\left[\bar{\boldsymbol{\Omega}}\right]_\times \delta\mathbf{v} - 2[\delta\boldsymbol{\Omega}]_\times \delta\mathbf{v}$$
$$- \left(\left[\bar{\boldsymbol{\Omega}}\right]_\times\right)^2 \bar{\mathbf{r}} - \left[\bar{\boldsymbol{\Omega}}\right]_\times [\delta\boldsymbol{\Omega}]_\times \bar{\mathbf{r}} - [\delta\boldsymbol{\Omega}]_\times \left[\bar{\boldsymbol{\Omega}}\right]_\times \bar{\mathbf{r}}$$
$$- ([\delta\boldsymbol{\Omega}]_\times)^2 \bar{\mathbf{r}} - \left(\left[\bar{\boldsymbol{\Omega}}\right]_\times\right)^2 \delta\mathbf{r} - \left[\bar{\boldsymbol{\Omega}}\right]_\times [\delta\boldsymbol{\Omega}]_\times \delta\mathbf{r}$$
$$- [\delta\boldsymbol{\Omega}]_\times \left[\bar{\boldsymbol{\Omega}}\right]_\times \delta\mathbf{r} - ([\delta\boldsymbol{\Omega}]_\times)^2 \delta\mathbf{r}$$
$$(A.7)$$

By eliminating the same terms in (A.6) and (A.7) and the second order terms and recognizing some cross-products (with $[\mathbf{a}]_\times \mathbf{b} = -[\mathbf{b}]_\times \mathbf{a}$ and $[\mathbf{a}]_\times [\mathbf{b}]_\times \mathbf{c} + [\mathbf{b}]_\times [\mathbf{c}]_\times \mathbf{a} + [\mathbf{c}]_\times [\mathbf{a}]_\times \mathbf{b} = \mathbf{0}$), we get:

$$\delta\dot{\mathbf{v}} = \bar{\mathbf{R}}\delta\mathbf{a}_s - \bar{\mathbf{R}}[\bar{\mathbf{a}}_s]_\times \delta\boldsymbol{\theta} - \delta\mathbf{a}_o + 2[\bar{\mathbf{v}}]_\times \delta\boldsymbol{\Omega} - 2\left[\bar{\boldsymbol{\Omega}}\right]_\times \delta\mathbf{v}$$
$$+ \left[\bar{\boldsymbol{\Omega}}\right]_\times [\bar{\mathbf{r}}]_\times \delta\boldsymbol{\Omega} - \left(-\left[\bar{\boldsymbol{\Omega}}\right]_\times [\bar{\mathbf{r}}]_\times + [\bar{\mathbf{r}}]_\times \left[\bar{\boldsymbol{\Omega}}\right]_\times\right)\delta\boldsymbol{\Omega}$$
$$- \left(\left[\bar{\boldsymbol{\Omega}}\right]_\times\right)^2 \delta\mathbf{r}$$
$$(A.8)$$

By rearranging the terms and using (A.3), we finally obtain:

$$\delta\dot{\mathbf{v}} = -\left(\left[\tilde{\boldsymbol{\Omega}} - \mathbf{b}_\Omega\right]_\times\right)^2 \delta\mathbf{r} - 2\left[\tilde{\boldsymbol{\Omega}} - \mathbf{b}_\Omega\right]_\times \delta\mathbf{v}$$
$$- \bar{\mathbf{R}}[\tilde{a}_s]_\times \delta\boldsymbol{\theta} - \left(2[\bar{\mathbf{v}}]_\times + 2\left[\tilde{\boldsymbol{\Omega}} - \mathbf{b}_\Omega\right]_\times [\bar{\mathbf{r}}]_\times\right.$$
$$\left. - [\bar{\mathbf{r}}]_\times \left[\tilde{\boldsymbol{\Omega}} - \mathbf{b}_\Omega\right]_\times\right)\delta\mathbf{b}_\Omega - \bar{\mathbf{R}}\mathbf{n}_{a_s} + \mathbf{n}_{a_o}$$
$$- \left(2[\bar{\mathbf{v}}]_\times + 2\left[\tilde{\boldsymbol{\Omega}} - \mathbf{b}_\Omega\right]_\times [\bar{\mathbf{r}}]_\times - [\bar{\mathbf{r}}]_\times \left[\tilde{\boldsymbol{\Omega}} - \mathbf{b}_\Omega\right]_\times\right)\mathbf{n}_\Omega$$
$$(A.9)$$

If the accelerometer noise is white, uncorrelated and isotropic this expression can be further simplified since $\mathbb{E}\left[\mathbf{n}_{a_s}\right] = 0$, $\mathbb{E}\left[\mathbf{n}_{a_s}\mathbf{n}_{a_s}^{\mathrm{T}}\right] = \sigma_{a_s}^2\mathbf{I}$ and we obtain $\bar{\mathbf{R}}\mathbf{n}_{a_s} = \mathbf{n}_{a_s}$

Appendix B. THE ATTITUDE ERROR DERIVATION

This derivation is entirely inspired to the work Sola (2017). We want to obtain the dynamics of the angular errors $\delta\dot{\boldsymbol{\theta}}$ by starting from the true and the nominal kinematics of the quaternions:

$$\dot{\mathbf{q}} = \frac{1}{2}\mathbf{q}\otimes\left(\boldsymbol{\omega} - \mathbf{R}^{\mathrm{T}}\boldsymbol{\Omega}\right) \tag{B.1}$$

$$\dot{\bar{\mathbf{q}}} = \frac{1}{2}\bar{\mathbf{q}}\otimes\left(\bar{\boldsymbol{\omega}} - \bar{\mathbf{R}}^{\mathrm{T}}\bar{\boldsymbol{\Omega}}\right) \tag{B.2}$$

The true value of the rotation matrix $\mathbf{R}$ is given by (A.1).

For the angular rates we can write:

$$\begin{cases} \bar{\boldsymbol{\Omega}} \triangleq \tilde{\boldsymbol{\Omega}} - \mathbf{b}_\Omega \\ \delta\boldsymbol{\Omega} \triangleq -\delta\mathbf{b}_\Omega - \mathbf{n}_\Omega \end{cases} \begin{cases} \bar{\boldsymbol{\omega}} \triangleq \tilde{\boldsymbol{\omega}} - \mathbf{b}_\omega \\ \delta\boldsymbol{\omega} \triangleq -\delta\mathbf{b}_\omega - \mathbf{n}_\omega \end{cases} \tag{B.3}$$

We compute $\dot{\mathbf{q}}$ in two ways as done in Sola (2017):

$$\frac{d}{dt}\left(\bar{\mathbf{q}}\otimes\delta\mathbf{q}\right) = \frac{1}{2}\mathbf{q}\otimes\left(\boldsymbol{\omega} - \mathbf{R}^{\mathrm{T}}\boldsymbol{\Omega}\right) \tag{B.4}$$

$$\dot{\bar{\mathbf{q}}}\otimes\delta\mathbf{q} + \bar{\mathbf{q}}\otimes\delta\dot{\mathbf{q}} = \frac{1}{2}\bar{\mathbf{q}}\otimes\delta\mathbf{q}\otimes\left(\boldsymbol{\omega} - \mathbf{R}^{\mathrm{T}}\boldsymbol{\Omega}\right) \tag{B.5}$$

$$\frac{1}{2}\bar{\mathbf{q}}\otimes\left(\bar{\boldsymbol{\omega}} - \bar{\mathbf{R}}^{\mathrm{T}}\bar{\boldsymbol{\Omega}}\right)\otimes\delta\mathbf{q} + \bar{\mathbf{q}}\otimes\delta\dot{\mathbf{q}} = \frac{1}{2}\bar{\mathbf{q}}\otimes\delta\mathbf{q}\otimes\left(\boldsymbol{\omega} - \mathbf{R}^{\mathrm{T}}\boldsymbol{\Omega}\right) \tag{B.6}$$

By simplifying $\bar{\mathbf{q}}$:

$$\left(\bar{\boldsymbol{\omega}} - \bar{\mathbf{R}}^{\mathrm{T}}\bar{\boldsymbol{\Omega}}\right)\otimes\delta\mathbf{q} + 2\delta\dot{\mathbf{q}} = \delta\mathbf{q}\otimes\left(\boldsymbol{\omega} - \mathbf{R}^{\mathrm{T}}\boldsymbol{\Omega}\right) \tag{B.7}$$

The right side of (B.7) can be developed as:

$$\delta\mathbf{q}\otimes\left(\boldsymbol{\omega} - \mathbf{R}^{\mathrm{T}}\boldsymbol{\Omega}\right) = \delta\mathbf{q}\otimes\left(\boldsymbol{\omega} - \left(\mathbf{I} + [\delta\boldsymbol{\theta}]_\times\right)^{\mathrm{T}}\bar{\mathbf{R}}^{\mathrm{T}}\left(\bar{\boldsymbol{\Omega}} + \delta\boldsymbol{\Omega}\right)\right)$$
$$= \delta\mathbf{q}\otimes\left(\boldsymbol{\omega} - \bar{\mathbf{R}}^{\mathrm{T}}\bar{\boldsymbol{\Omega}} - \bar{\mathbf{R}}^{\mathrm{T}}\delta\boldsymbol{\Omega} + [\delta\boldsymbol{\theta}]_\times\bar{\mathbf{R}}^{\mathrm{T}}\bar{\boldsymbol{\Omega}} + [\delta\boldsymbol{\theta}]_\times\bar{\mathbf{R}}^{\mathrm{T}}\delta\boldsymbol{\Omega}\right) \tag{B.8}$$

Note that $[\delta\boldsymbol{\theta}]_\times\bar{\mathbf{R}}^{\mathrm{T}}\bar{\boldsymbol{\Omega}} = -\left[\bar{\mathbf{R}}^{\mathrm{T}}\bar{\boldsymbol{\Omega}}\right]_\times\delta\boldsymbol{\theta}$ and the second-order terms can be neglected. We can then rewrite (B.7):

$$\left(\bar{\boldsymbol{\omega}} - \bar{\mathbf{R}}^{\mathrm{T}}\bar{\boldsymbol{\Omega}}\right)\otimes\delta\mathbf{q} + 2\delta\dot{\mathbf{q}} =$$
$$= \delta\mathbf{q}\otimes\left(\boldsymbol{\omega} - \bar{\mathbf{R}}^{\mathrm{T}}\bar{\boldsymbol{\Omega}} - \bar{\mathbf{R}}^{\mathrm{T}}\delta\boldsymbol{\Omega} - \left[\bar{\mathbf{R}}^{\mathrm{T}}\bar{\boldsymbol{\Omega}}\right]_\times\delta\boldsymbol{\theta}\right) \tag{B.9}$$

By isolating $\delta\dot{\mathbf{q}}$:

$$\begin{bmatrix}0 \\ \delta\dot{\boldsymbol{\theta}}\end{bmatrix} = 2\delta\dot{\mathbf{q}} = \delta\mathbf{q}\otimes\left(\boldsymbol{\omega} - \bar{\mathbf{R}}^{\mathrm{T}}\bar{\boldsymbol{\Omega}} - \bar{\mathbf{R}}^{\mathrm{T}}\delta\boldsymbol{\Omega} - \left[\bar{\mathbf{R}}^{\mathrm{T}}\bar{\boldsymbol{\Omega}}\right]_\times\delta\boldsymbol{\theta}\right)$$
$$- \left(\bar{\boldsymbol{\omega}} - \bar{\mathbf{R}}^{\mathrm{T}}\bar{\boldsymbol{\Omega}}\right)\otimes\delta\mathbf{q} \tag{B.10}$$

Let's take:

$$\begin{cases} \mathbf{A} = \boldsymbol{\omega} - \bar{\mathbf{R}}^{\mathrm{T}}\bar{\boldsymbol{\Omega}} - \bar{\mathbf{R}}^{\mathrm{T}}\delta\boldsymbol{\Omega} - \left[\bar{\mathbf{R}}^{\mathrm{T}}\bar{\boldsymbol{\Omega}}\right]_\times\delta\boldsymbol{\theta} \\ \mathbf{B} = \bar{\boldsymbol{\omega}} - \bar{\mathbf{R}}^{\mathrm{T}}\bar{\boldsymbol{\Omega}} \end{cases} \tag{B.11}$$

Equation (B.10) becomes:

$$\begin{bmatrix}0 \\ \delta\dot{\boldsymbol{\theta}}\end{bmatrix} = 2\delta\dot{\mathbf{q}} = \delta\mathbf{q}\otimes\mathbf{A} - \mathbf{B}\otimes\delta\mathbf{q} =$$
$$= \begin{bmatrix}0 & -(\mathbf{A}-\mathbf{B})^{\mathrm{T}} \\ (\mathbf{A}-\mathbf{B}) & -[\mathbf{A}+\mathbf{B}]_\times\end{bmatrix}\begin{bmatrix}1 \\ \delta\boldsymbol{\theta}/2\end{bmatrix} + \mathcal{O}\left(||\delta\boldsymbol{\theta}||^2\right) \tag{B.12}$$

which results in one scalar and one vector equalities:

$$0 = \left(\delta\boldsymbol{\omega} - \bar{\mathbf{R}}^{\mathrm{T}}\delta\boldsymbol{\Omega} - \left[\bar{\mathbf{R}}^{\mathrm{T}}\bar{\boldsymbol{\Omega}}\right]_\times\delta\boldsymbol{\theta}\right)^{\mathrm{T}}\delta\boldsymbol{\theta} + \mathcal{O}\left(|\delta\boldsymbol{\theta}|^2\right) \tag{B.13}$$

$$\delta\dot{\boldsymbol{\theta}} = \delta\boldsymbol{\omega} - \bar{\mathbf{R}}^{\mathrm{T}}\delta\boldsymbol{\Omega} - \left[\bar{\mathbf{R}}^{\mathrm{T}}\bar{\boldsymbol{\Omega}}\right]_\times\delta\boldsymbol{\theta} - \frac{1}{2}\left[2\bar{\boldsymbol{\omega}} + \delta\boldsymbol{\omega} - 2\bar{\mathbf{R}}^{\mathrm{T}}\bar{\boldsymbol{\Omega}}\right.$$
$$\left. - \bar{\mathbf{R}}^{\mathrm{T}}\delta\boldsymbol{\Omega} + - \left[\bar{\mathbf{R}}^{\mathrm{T}}\bar{\boldsymbol{\Omega}}\right]_\times\delta\boldsymbol{\theta}\right]_\times\delta\boldsymbol{\theta} + \mathcal{O}\left(||\delta\boldsymbol{\theta}||^2\right) \tag{B.14}$$

Equation (B.13) can be neglected since it is formed by only second-order infinitesimal terms. After neglecting all second-order terms, the second equation (B.14) can be rewritten as:

$$\delta\dot{\boldsymbol{\theta}} = -[\bar{\boldsymbol{\omega}}]_\times\delta\boldsymbol{\theta} + \delta\boldsymbol{\omega} - \bar{\mathbf{R}}^{\mathrm{T}}\delta\boldsymbol{\Omega} \tag{B.15}$$

and finally the linearized dynamics of the angular error is obtained by using (B.3):

$$\delta\dot{\boldsymbol{\theta}} = -\left[\tilde{\boldsymbol{\omega}} - \mathbf{b}_\omega\right]_\times\delta\boldsymbol{\theta} + \bar{\mathbf{R}}^{\mathrm{T}}\delta\mathbf{b}_\Omega - \delta\mathbf{b}_\omega + \bar{\mathbf{R}}^{\mathrm{T}}\mathbf{n}_\Omega - \mathbf{n}_\omega \tag{B.16}$$

If the gyrometer noise is white, uncorrelated and isotropic $\bar{\mathbf{R}}^{\mathrm{T}}\mathbf{n}_\Omega = \mathbf{n}_\Omega$ and (B.16) then becomes:

$$\delta\dot{\boldsymbol{\theta}} = -\left[\tilde{\boldsymbol{\omega}} - \mathbf{b}_\omega\right]_\times\delta\boldsymbol{\theta} + \bar{\mathbf{R}}^{\mathrm{T}}\delta\mathbf{b}_\Omega - \delta\mathbf{b}_\omega + \mathbf{n}_\Omega - \mathbf{n}_\omega \tag{B.17}$$

REFERENCES

Comellini, A., Casu, D., Zenou, E., Dubanchet, V., and Espinosa, C. (2020). Incorporating delayed and multi-rate measurements in navigation filter for autonomous space rendezvous. *Journal of Guidance, Control, and Dynamics*, 43(6), 1164–1172.

Dubois, L., Evain, H., Meyniel, V., Alazard, D., and Rognant, M. (2020). Design of a steering law for control moment gyro clusters based on a set of initial positions. *IFAC-PapersOnLine*, 53(2), 14851–14856.

Evain, H., Alazard, D., Rognant, M., Solatges, T., Brunet, A., Mignot, J., Rodriguez, N., and Dias-Ribeiro, A. (2019). Satellite attitude control with a six-control moment gyro cluster tested under microgravity conditions. In *International Symposium on Space Flight Dynamics 2019 (ISSFD)*, 1387–1392. Melbourne, AU. URL https://oatao.univ-toulouse.fr/23902/.

Evain, H., Solatges, T., Brunet, A., Dias Ribeiro, A., Sipile, L., Rognant, M., Alazard, D., and Mignot, J. (2017). Design and control of a nano-control moment gyro cluster for experiments in a parabolic flight campaign. In *IFAC World Congress*.

Kassarian, E., Rognant, M., Evain, H., Alazard, D., and Chauffaut, C. (2020). Convergent ekf-based control allocation: general formulation and application to a control moment gyro cluster. In *2020 American Control Conference (ACC)*, 4454–4459. doi: 10.23919/ACC45564.2020.9147333.

Simon, D. (2006). *Optimal state estimation: Kalman, H infinity, and nonlinear approaches*. John Wiley & Sons.

Sola, J. (2017). Quaternion kinematics for the error-state kalman filter. *arXiv preprint arXiv:1711.02508*.